Environmental Effects in Kelvin Force Microscopy of Modified Diamond Surfaces

W.W.R. ARAUJO,[1] M.C. SALVADORI,[1]* F.S. TEIXEIRA,[1] M. CATTANI,[1] AND I.G. BROWN[2]
[1]*Institute of Physics, University of São Paulo, C.P. 66318, CEP 05315-970, São Paulo S.P., Brazil*
[2]*Lawrence Berkeley National Laboratory, 1 Cyclotron Road, Berkeley, California 94720*

KEY WORDS diamond film; Kelvin force microscopy; surface characterization; surface microscopy; surface electronic properties

ABSTRACT We have explored the effects of atmospheric environment on Kelvin force microscopy (KFM) measurements of potential difference between different regions of test polycrystalline diamond surfaces. The diamond films were deposited by microwave plasma-assisted chemical vapor deposition, which naturally produces hydrogen terminations on the surface of the films formed. Selected regions were patterned by electron-beam lithography and chemical terminations of oxygen or fluorine were created by exposure to an oxygen or fluorine plasma source. For KFM imaging, the samples were mounted in a hood with a constant flow of helium gas. Successive images were taken over a 5-h period showing the effect of the environment on KFM imaging. We conclude that the helium flow removes water molecules adsorbed on the surface of the samples, resulting in differences in surface potential between adjacent regions. The degree of water removal is different for surfaces with different terminations. The results highlight the importance of taking into account the atmospheric environment when carrying out KFM analysis. *Microsc. Res. Tech. 75:977–981, 2012.*

INTRODUCTION

Kelvin force microscopy (KFM), one of a number of scanning probe microscopy (SPM) techniques, is a powerful imaging method that provides information about the potential difference between adjacent regions on a surface. SPM techniques, including KFM, are commonly carried out under ambient conditions (Rezek and Nebel, 2005; Tachiki et al., 2005), although there are also high vacuum versions (Pakes et al., 2009). It is known that control of the ambient is necessary for surface potential measurements due to the adsorbed water layer on the surface, since it shields the surface potential (Sugimura et al., 2002). It is also known that surface chemistry influences the surface potential (Barth et al., 2011; Ertl et al., 1982; Ladas et al., 1989; Shimizu et al., 2008). To avoid the undesired effects of adsorbed water molecules (Rezek et al., 2004), a flow of dry gas is usually applied (Ono et al., 2001; Zaghloul et al., 2011). In the work described here, we registered atomic force microscopy (AFM)/KFM images while eliminating the adsorbed moisture on the surface, observing the behavior of the surface potential difference. In this way we show dynamically the influence of a constant flow of dry helium on the KFM measurements.

MATERIALS AND METHODS

The equipment used for obtaining KFM images was a commercial SPM, Nanoscope IIIa MultiMode™, with Extender™ electronics module from Digital Instruments, Santa Barbara, CA. With this device, the KFM image (surface potential map) is generated simultaneously with an AFM topographic image using the interleave mode. We used a metal-coated cantilever nanoprobe (MESP, Bruker AFM Probes) with resonant frequency ~60-80 kHz. Initially, the AFM/KFM images of the surface were obtained under laboratory ambient conditions. The AFM/KFM measurements were then repeated and stored over a period of 5 h with a flow of 1 L/min of dry gas. The gas used for the KFM measurements was helium. In this procedure, a controlled atmosphere hood was used—basically an acrylic box (Veeco Multimode atmospheric hood cap MMAHC) covering the entire instrument (scanner head, cantilever, and sample) with gas input and output.

We used the interleaved mode for AFM and KFM acquisition. In this mode, for each scan line the probe first measures the surface topography using the AFM intermittent contact mode. Once the topography is obtained for a scan line, the tip is lifted from the surface by a few tens of nanometers (typically ~50 nm) and scans the same line again, following the just-measured topography, registering the value of the surface potential for each point (x, y).

In the AFM intermittent contact mode, used for obtaining the surface topography image, a transducer vibrates the cantilever at or very close to its resonance frequency ω so it oscillates at maximum amplitude. Due to variations in surface height, the amplitude varies and the system makes corrections in height so as to maintain constant surface/tip separation. Thus a

*Correspondence to: Cecilia Salvadori, Institute of Physics, University of São Paulo, C.P. 66318, CEP 05315-970, São Paulo S.P., Brazil.
E-mail: mcsalva@if.usp.br

Received 8 January 2012; accepted in revised form 23 January 2012

Contract grant sponsors: Fundação de Amparo a Pesquisa do Estado de São Paulo (FAPESP), Conselho Nacional de Desenvolvimento Científico e Tecnológico (CNPq), Brazil.

DOI 10.1002/jemt.22022

Published online 7 March 2012 in Wiley Online Library (wileyonlinelibrary.com).

height is associated with each point and an image is generated when a complete area is scanned.

For the surface potential measurements (Multimode manual, 2004; Nonnenmacher et al., 1991; Palermo et al., 2006) the tip must be conducting and the sample grounded. The tip and the surface have different values of work function, φ_{tip} and $\varphi_{surface}$, respectively, and they are separated by the lift height z, forming a simple capacitor. The voltage difference between tip and surface is given by

$$\frac{\Delta\varphi}{e} = \frac{\varphi_{surface}}{e} - \frac{\varphi_{tip}}{e}$$

where e is the electron charge. Then an oscillatory voltage $V_{ac} = V_a \sin\omega t$ is applied to the tip by the microscope system. Note that the oscillation frequency ω of the applied voltage is at, or very close to, the mechanical resonance frequency of the cantilever. The tip interacts electrostatically with the surface, being attracted and repelled at the same applied frequency and generates an oscillating electric force at frequency ω which causes mechanical oscillation in the cantilever that can be detected. By adding a dc potential difference V_{dc} between tip and surface, so that the tip reaches the surface potential ($V_{dc} = \Delta\varphi/e$), the electrostatic interaction is minimized and the cantilever oscillation amplitude decreases to a minimum value. The applied voltage V_{dc} is recorded for each point (x,y) of the scan.

The technique can be analyzed by considering the tip/surface capacitor with total voltage given by

$$\Delta V = \frac{\Delta\varphi}{e} - V_{dc} + V_a \sin(\omega t)$$

The energy U stored in the capacitor is $U = 1/2C\Delta V^2$, where C is the local capacitance between tip and sample. There is an electrostatic force between tip and sample due to the capacitance between them that depends on their separation (Jacobs et al., 1998), and which is given in terms of the tip/sample separation z as

$$F = \frac{\partial U}{\partial z} = -\frac{1}{2}\frac{\partial C}{\partial z}\Delta V^2 = F_{dc} + F_\omega + F_{2\omega}$$

where

$$F_{dc} = -\frac{1}{2}\frac{\partial C}{\partial z}\left[\left(\frac{\Delta\varphi}{e} - V_{dc}\right)^2 + \frac{V_{ac}^2}{2}\right]$$

$$F_\omega = -\frac{\partial C}{\partial z}\left[\left(\frac{\Delta\varphi}{e} - V_{dc}\right)V_{ac}\sin(\omega t)\right]$$

$$F_{2\omega} = \frac{1}{4}\frac{\partial C}{\partial z}\left[V_{ac}^2\cos(2\omega t)\right].$$

Noting the terms F_{dc} and F_ω, it is clear that the minimum force magnitude occurs for $V_{dc} = \Delta\varphi/e$. Thus $\Delta\varphi/e$ can be obtained by increasing V_{dc} to produce minimum oscillation amplitude.

The samples used in this work were diamond films whose surfaces were modified by a plasma treatment to generate adjacent regions of different surface potential. Polycrystalline diamond films were synthesized by microwave plasma-assisted chemical vapor deposition (MPACVD) (Salvadori et al., 1995). The films were deposited onto polished n-type [100] silicon wafers with dimensions 17 mm × 17 mm and thickness about 0.3 mm. The deposition parameters were: substrate temperature 850°C, pressure 50 Torr, hydrogen flow rate 300 sccm, methane flow rate 3 sccm, and nitrogen flow rate 3 sccm. A typical deposition was carried out for 24 h. The diamond films presented clusters of nanocrystals of size about 20 nm as observed by X-ray diffraction; the film thickness was about 10 μm and the surface roughness about 90 nm, as previously reported (Salvadori et al., 2010). The MPACVD process naturally produces hydrogen terminations on the surface of the films formed, since the gas mixture used in the synthesis contain basically carbon and hydrogen. We made three different samples having adjacent regions with terminations of hydrogen/fluorine, or hydrogen/oxygen or fluorine/oxygen. To do this, the diamond film surfaces were first spin-coated with polymethylmethacrylate (PMMA) with molecular weight 950,000 purchased from Allresist. The surfaces were then electron-beam lithographed so as to form patterns on the surface with some regions remaining protected by the PMMA. The samples were exposed to an oxygen (5 min) or a sulfur hexafluoride (9 min) plasma stream, thereby replacing the surface hydrogen terminations by oxygen or fluorine terminations, respectively, in the regions exposed by the lithography. In this way, we produced samples with adjacent regions containing hydrogen/oxygen and hydrogen/fluorine terminations. For the case of the fluorine-/oxygen-terminated sample, first an entire sample surface was exposed to sulfur hexafluoride plasma for 5 min, and then the sample was lithographed, as just described, and exposed to an oxygen plasma stream for 3 min. These processing times were chosen based on our previous experience (Salvadori et al., 2010) in optimizing the surface potential. A hollow-cathode plasma gun was used (Vizir et al., 2007) for the plasma treatment. For the oxygen plasma, the gun was operated at a voltage of about 750 V dc and a vacuum chamber pressure of 2.0×10^{-4} Torr, with the sample positioned 120 mm from the plasma gun. For the fluorine plasma, the gun was fed with sulfur hexafluoride gas, SF_6, at an operating voltage of about 800 V dc and a pressure of 7.5×10^{-3} Torr, with the sample positioned 15 mm from the plasma gun exit. After the plasmas treatment, the PMMA was completely removed from the samples by an ultrasonic bath with acetone and isopropyl alcohol, in sequence.

For KFM imaging, we used a lift height of 50 nm, amplitude $V_a = 6$ V, scan size 150 μm, and scan rate 1 Hz. We obtained one KFM image every 14 min over a total of 5 h in helium flow. For each image, three potential profiles allowed calculation of the average potential difference between adjacent regions with different terminations.

RESULTS

Figures 1a and 1b show AFM and KFM images, respectively, for the hydrogen/fluorine sample under

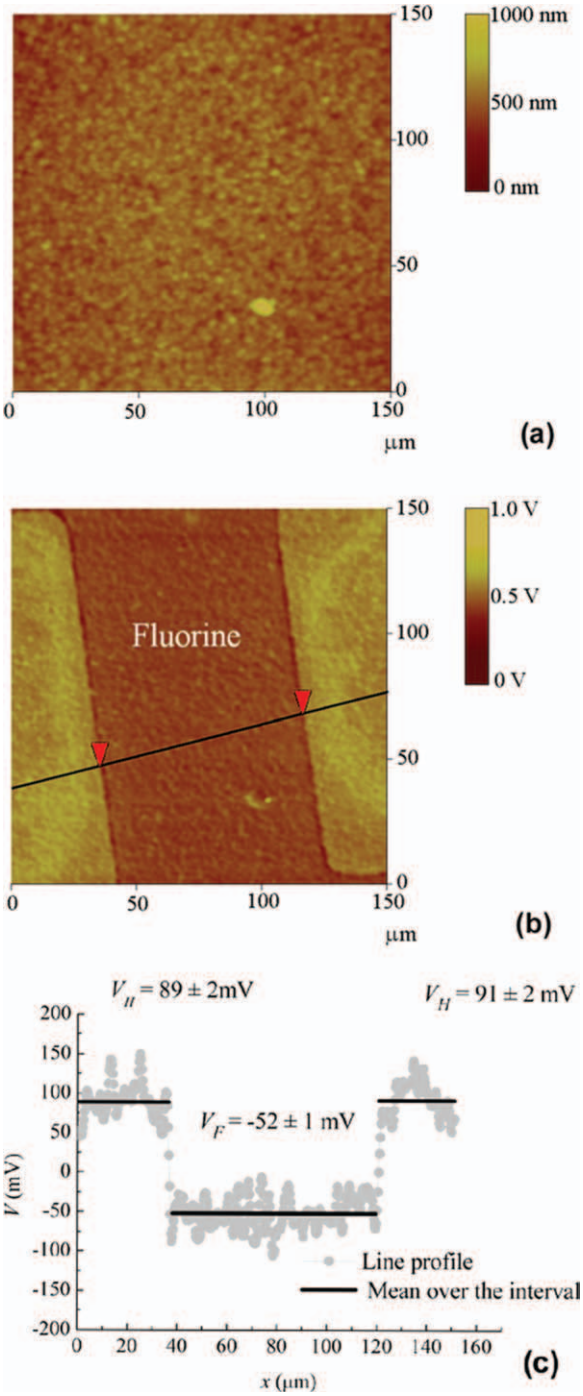

Fig. 1. **(a)** AFM and (**b**) KFM images of polycrystalline diamond surface with adjacent regions with hydrogen and fluorine terminations, under ambient environmental acquisition conditions. **(c)** Potential profile along the line traced in the KFM image. [Color figure can be viewed in the online issue, which is available at wileyonlinelibrary.com.]

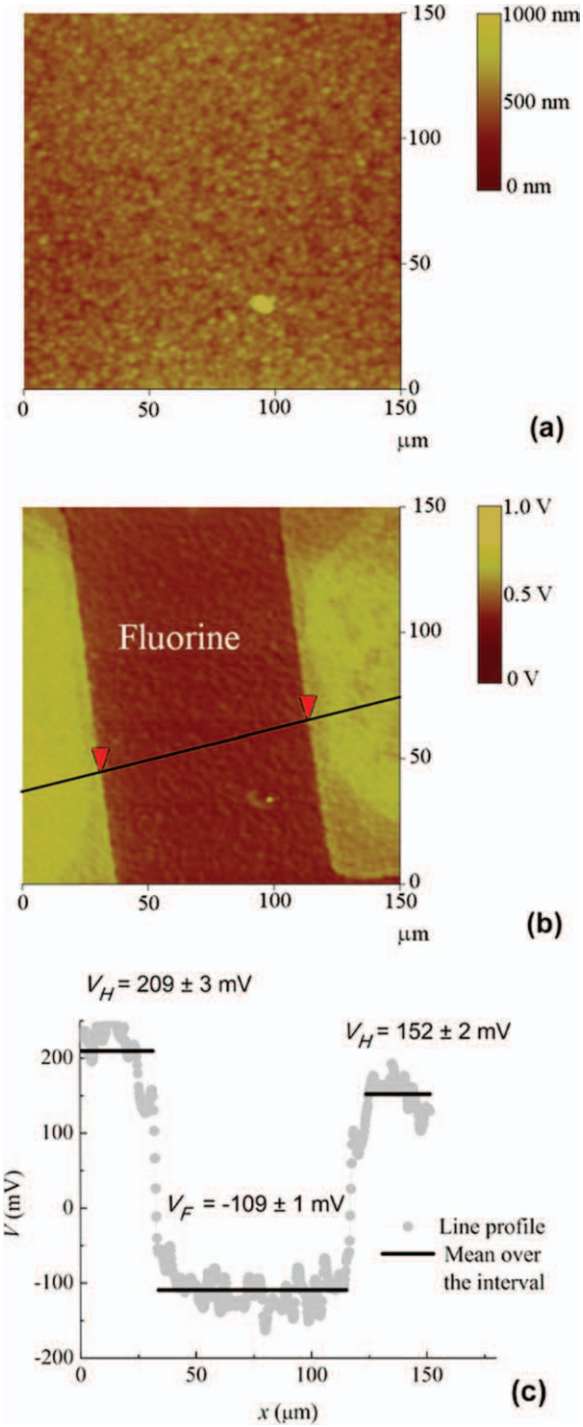

Fig. 2. **(a)** AFM and (**b**) KFM images of polycrystalline diamond surface with adjacent regions with hydrogen and fluorine terminations, after 5 h in helium flow. **(c)** Potential profile along the line traced in the KFM image. [Color figure can be viewed in the online issue, which is available at wileyonlinelibrary.com.]

ambient conditions. Figure 1c shows the potential profile along the line traced in the KFM image as shown in Figure 1b. In this potential profile, we obtain averages as shown by the horizontal lines drawn for each different region, thus defining a local potential and its uncertainty. For regions with the same terminations the associated potential was taken as an average; for example, in the case of Figure 1c the surface potential with hydrogen termination was measured in two regions, giving 89 mV and 91 mV for an average of 90 mV. In this way, the potential difference between

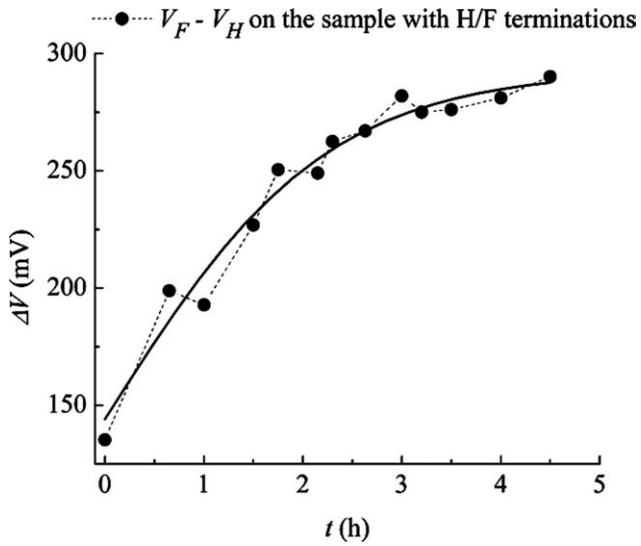

Fig. 3. Potential difference between regions with hydrogen and fluorine terminations as a function of exposure time to helium flow. The experimental data are represented by filled circles and the continuous line is a best-fit showing the exponential behavior of the data.

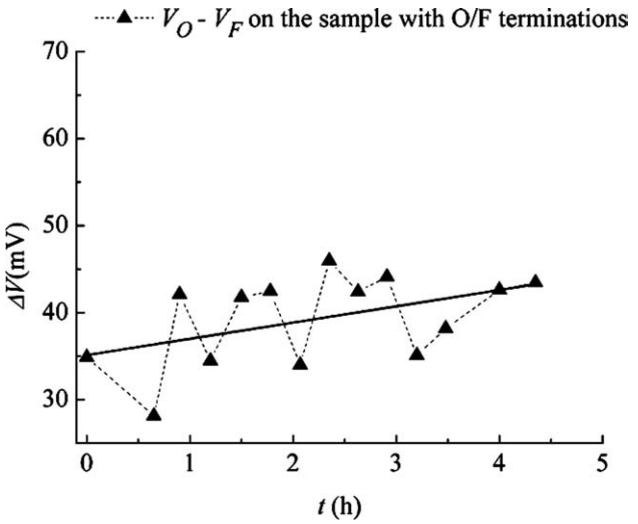

Fig. 5. Potential difference between regions with fluorine and oxygen terminations as a function of exposure time to helium flow. The experimental data are represented by filled circles and the continuous line is a best-fit showing the linear behavior of the data.

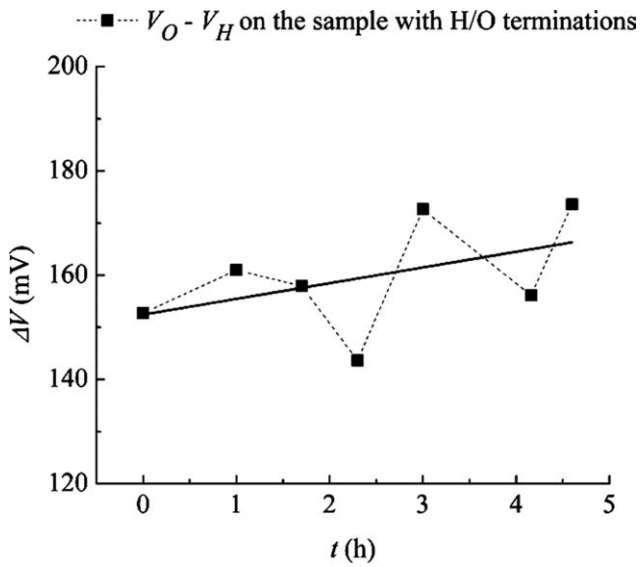

Fig. 4. Potential difference between regions with hydrogen and oxygen terminations as a function of exposure time to helium flow. The experimental data are represented by filled circles and the continuous line is a best-fit showing the linear behavior of the data.

regions with fluorine and hydrogen terminations in the profile of Figure 1c was obtained as $V_F - V_H = 142 \pm 3$ mV. We measured three profiles in three different places in the KFM image of Figure 1b, and the average potential difference between regions with fluorine and hydrogen terminations was found to be $V_F - V_H = 135 \pm 7$ mV.

Figures 2a and 2b show AFM and KFM images, respectively, for the same hydrogen/fluorine sample after 5 h in helium flow. The potential profile clearly indicates an increase of the potential difference between the two regions compared with the results obtained as in Figure 1c (i.e., the same sample measured under ambient conditions).

Figure 3 shows the measured mean potential difference between regions with hydrogen and fluorine terminations as a function of time for which the sample was exposed to continuous helium flow; the experimental data are represented by filled circles and the continuous line shows the exponential curve $\Delta V = c - e^{-at}$, where c and a are constants (chosen here for best fit). As mentioned above, the potential difference between regions with hydrogen/fluorine terminations under ambient conditions was 135 ± 7 mV. After 3 h in helium atmosphere the potential difference has saturated at an average value of 280 ± 8 mV (mean of the last five values in Fig. 3)—an increase of 107% above that under ambient conditions. The procedure for obtaining each point shown in Figure 3 was basically the same as described.

Figures 4 and 5 show the mean potential differences between regions with hydrogen and oxygen terminations, and with fluorine and oxygen terminations, respectively, as a function of time for which the samples were exposed to continuous helium flow. One can see an approximately linear increase in the potential difference with time for both cases. For the hydrogen/oxygen terminated surface, the potential difference under ambient conditions was 153 ± 5 mV, increasing by 5%, after 5 h in helium flow. For the fluorine/oxygen terminated surface, the potential difference under ambient conditions was 35 ± 1 mV, increasing by 17% after 5 h in helium flow.

We have reported prior work (Salvadori et al., 2010) indicating the contact angle (with deionized pure water) of diamond surfaces terminated by fluorine (93°), hydrogen (83°), and oxygen (75°). We can associate these prior results with the results obtained here with flowing helium gas during KFM measurements. Surfaces with hydrogen/fluorine terminations are relatively hydrophobic, allowing easier removal of the layer

of water adsorbed on the surface. Thus here we found that the potential difference increased (exponentially) by as much as 107%. However surfaces with hydrogen/oxygen and fluorine/oxygen terminations are more hydrophilic, and it is more difficult to remove the layer of water adsorbed on the surface. This is consistent with our observations reported here that the potential difference exhibits only a small (linear) growth, with gains of 5% and 17%, respectively.

CONCLUSION

Our KFM measurements show the influence of environmental moisture shielding the surface potential of MAPCVD diamond film surfaces. The samples were mounted in a suitable hood with a constant flow of 1 L/min of helium gas, and images taken over a 5 h period under continuous helium gas flow, to study the environmental effect on KFM imaging. The potential difference increased by 107%, from 135 mV to 280 mV, for neighboring surface regions with hydrogen and fluorine terminations, and by 5% and 17% for neighboring surface regions with hydrogen/oxygen and fluorine/oxygen terminations, respectively. These results imply that it is more difficult to remove the water layer adsorbed on the surface when the surface is terminated with oxygen (a more hydrophilic surface), and point out the need for carrying out the KFM in a flow of dry gas.

REFERENCES

Barth C, Foster AS, Henry CR, Shluger AL. 2011. Recent trends in surface characterization and chemistry with high-resolution scanning force methods. Adv Mater 23:477–501.

Ertl G, Norton PR, Rüstig J. 1982. Kinetic oscillations in the platinum-catalyzed oxidation of Co. Phys Rev Lett 49:177–180.

Jacobs HO, Leuchtmann P, Homan OJ, Stemmer A. 1998. Resolution and contrast in Kelvin probe force microscopy. Appl Phys 84: 1168–1174.

Ladas S, Imbihl R, Ertl G. 1989. Kinetic oscillations during the catalytic CO oxidation on Pd(110): The role of subsurface oxygen. Surf Sci 219:88–106.

Multimode SPM Instruction Manual, Revision E. 2004.

Nonnenmacher M, O'Boyle MP, Wickramasinghe HK. 1991. Kelvin probe force microscopy. Appl Phys Lett 58:2921–2923.

Ono S, Takeuchi M, Takahashi T. 2001. Kelvin probe force microscopy on InAs thin films grown on GaAs giant step structures formed on (110) GaAs vicinal substrates. Appl Phys Lett 78:1086–1089.

Pakes CI, Hoxley D, Rabeau JR, Edmonds MT, Kalish R, Prawer S. 2009. Scanning Kelvin-probe study of the hydrogen-terminated diamond surface in ultrahigh vacuum. Appl Phys Lett 95:123108–123111.

Palermo V, Palma M, Samori P. 2006. Electronic characterization of organic thin films by Kelvin Probe Force Microscopy. Adv Mater 18:145–164.

Rezek B, Nebel CE, Stutzmann M. 2004. Hydrogenated diamond surfaces studied by atomic and Kelvin force microscopy. Diamond Relat Mater 13:740–745.

Rezek B, Nebel CE. 2005. Kelvin force microscopy on diamond surfaces and devices. Diamond Relat Mater 14:466–469.

Salvadori MC, Mammana VP, Martins OG, Degasperi FT. 1995. Plasma-assisted chemical vapour deposition in a tunable microwave cavity. Plasma Sources Sci Technol 4:489–494.

Salvadori MC, Araujo WWR., Teixeira FS, Cattani M, Pasquarelli A, Oks EM, Brown IG. 2010. Termination of diamond surfaces with hydrogen, oxygen and fluorine using a small, simple plasma gun. Diamond Relat Mater 19:324–328.

Shimizu TK, Mugarza A, Cerdá JI, Salmeron M. 2008. Structure and reactions of carbon and hydrogen on Ru(0001): A scanning tunneling microscopy study. J Chem Phys 129:244103–244110.

Sugimura H, Ishida Y, Hayashi K, Takai O, Nakagiri N. 2002. Potential shielding by the surface water layer in Kelvin probe force microscopy. Appl Phys Lett 80:1459–1462.

Tachiki M, Kaibara Y, Sumikawa Y, Shigeno M, Kanazawa H, Banno T, Song KS, Umezawa H, Kawarada H. 2005. Characterization of locally modified diamond surface using Kelvin probe force microscope. Surf Sci 581:207–212.

Vizir A, Oks EM, Salvadori MC, Teixeira FS, Brown IG. 2007. Small plasma source for materials application. Rev Sci Instrum 78: 086103-1–086103-2.

Zaghloul U, Bhushan B, Pons P, Papaioannou GJ, Coccetti F, Plana R. 2011. On the influence of environment gases, relative humidity and gas purification on dielectric charging/discharging processes in electrostatically driven MEMS/NEMS devices. Nanotechnology 22: 035705.